Ab Initio (Density Functional) Study of the Exchange Coupling Constant in Di-μ-oxo-Bridged Copper(II) Dimers: A Valence Bond/Broken Symmetry Approach

Catherine Blanchet-Boiteux and Jean-Marie Mouesca*

Laboratoire de Métalloprotéines, Magnétisme et Modèles Chimiques, Service de Chimie Inorganique et Biologique, Département de Recherche Fondamentale sur la Matière Condensée, CEA-Grenoble, 17 rue des Martyrs, 38054 Grenoble Cedex 9, France

Received: October 5, 1999; In Final Form: December 16, 1999

Exchange coupling constants for di-μ-oxo-bridged copper(II) dimers with varying Cu−O−Cu bond angles have been calculated by means of density functional, broken symmetry (BS) techniques. The surprinsingly large ferromagnetism recently computed by Ruiz et al. [*Chem. Commun.* **1998**, 2767] for such model complexes has been rationalized within the framework of Kahn's valence bond model of molecular magnetism, although with a new twist. In effect, by defining and using the quantity $\Delta P^2(d_{xz})$, the difference of squared copper triplet and BS spin populations, we show that Kahn's (supposedly) antiferromagnetic term can turn out ferromagnetic, as exemplified in a spectacular way for the title compound.

I. Introduction

One way currently explored to obtain novel permanent magnets is to chemically generate discrete complexes exhibiting interesting magnetic properties, especially ferromagnetism. This is the reason a large variety of molecules have been studied in the last three decades,[1] as ferromagnetically compounds belong to the minority case. In that respect, and by focusing on transition metal dimers bridged by organic atoms or ligands, the azido[2,3] (when bridging in the "end-on" fashion) or hydroxo[4,5] anions are known as being among the most efficient mediators of ferromagnetism.

An alternative way of research relies on theoretical (molecular magnetism modeling) and computational (ab initio quantum) chemistry. Quite recently,[6] in a systematic search for new ferromagnetic compounds, Ruiz et al. showed computationally (based on a broken symmetry (BS) approach[7,8]) that the di-μ-oxo-bridged Cu(II) dimer, with a Cu−O−Cu bond angle θ of 101°, exhibits an exceptionally strong ferromagnetic coupling constant ($J = +989$ cm^{-1}), using the Heisenberg Hamiltonian $H = -J\mathbf{S_1}\cdot\mathbf{S_2}$ and the B3-LYP method as implemented in the GAUSSIAN package[9] and by taking the energy of the broken-symmetry solution as an approximation to that of the singlet state (as proposed in ref 3). This last di-μ-oxo-bridged Cu(II) dimer thus becomes a potentially very interesting candidate in the run for ferromagnetically coupled compounds.

Unfortunately, there are no oxo-bridged Cu(II) dimers described in the literature. With alternative copper and/or bridge oxidation states, there are, however, Cu(I) μ-dioxygen-, Cu(II) μ-peroxo-, or Cu(III) di-μ-oxo-bridged dimers, all three being electronic isomers studied within the general context of dioxygen activation by copper sites in biological and catalytic (oxidases) systems[10−12] (and references therein). Interconversion can occur between these last isoelectronic forms, but they have all been shown to exhibit strong antiferromagnetism.

There are, however, a few published studies on homometallic (non-copper) di-μ-oxo dimers, both experimental[13] with Fe(III) and theoretical[14] with Mn(III/III), Mn(III/IV), and Mn(IV/IV). But these are measured or predicted to be antiferromagnetic.

Within the Hay−Thibeault−Hoffmann molecular orbital (HTH-MO) model,[15] the exchange coupling constant J of an A−X−B dimer (A and B are the metallic sites, and X the bridging unit) is decomposed into ferromagnetic (J_F) and antiferromagnetic (J_{AF}) contributions. More precisely, J_{AF} varies as $-\Delta^2/U$, where Δ stands as the singly occupied molecular orbitals (SOMOs) gap in the triplet state and U is the covalent A−B/ionic A^+-B^- gap. In this context, the di-oxo-bridged Cu(II) dimer was found by Ruiz et al. to present a near degeneracy of the two SOMOs. This reduces (or even cancels) the antiferromagnetic contribution to the total exchange coupling constant. More cannot be said as the study of ferromagnetic systems (where $|J_{AF}| < J_F$) cannot be undertaken within this MO formalism. In effect, J_F is usually assumed to be constant for a given family of compounds, and the variation of $J = J_F + J_{AF}$ is thus generally ascribed to J_{AF} through that of Δ.

Upon reconducting part of the above-mentioned computations by Ruiz et al., we came across some slightly differing quantitative results, especially concerning the case of the planar $[Cu_2(\mu\text{-}O)_2(NH_3)_4]^0$ cation (cf. Scheme 1). But we obtained strong ferromagnetism as well. Please notice that, as $S_{AB}^2 \leq 0.1$ in our computations (where S_{AB} is the overlap beween the localized magnetic orbitals of monomers A and B), we did not equate broken symmetry and singlet state energies. This amounts to obtaining J values twice as large as those computed by Ruiz et al.[6] (in anticipation to section III.2, we thus computed for $\theta = 101°$, $J = 1604$ cm^{-1}, which is 802 cm^{-1} in Ruiz et al.'s controversial convention[16]). Other reasons for the differences may lie in the fact that we used different exchange-correlation potentials, as proposed in the ADF quantum chemical code[17,18] (cf. section III.1) We also slightly modified the original ADF triple ζ copper basis set, spatially contracting it, in relation with other studies of ours.[19]

These last points are not, however, the main subject of this article. Our own computations gave us rather an opportunity to elaborate some new theoretical insights and results, reflecting on some of the sources of ferromagnetism not considered quantitatively so far. This may serve in turn as a guide to interpret Ruiz et al.'s very interesting results.[6]

10.1021/jp993535r CCC: $19.00
Published on Web 02/18/2000

SCHEME 1: Schematic Representation of the Studied Planar Oxo-Bridged Copper Dimer[a]

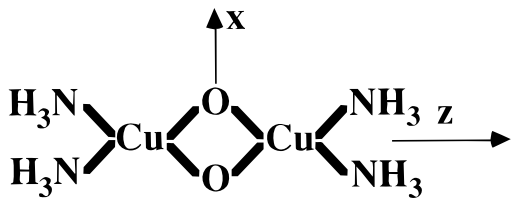

[a] The chosen axes are also indicated.

II. Valence Bond Description of Molecular Magnetism

II.1. Kahn and Briat's Model. Kahn and Briat's valence bond (KB-VB) approach[20,21] of molecular magnetism, the alternative to that of HTH(-MO), goes back to Heitler−London's view of the chemical bond, expressing the exchange term in term of localized (valence-bond) orbitals. Within the "active electron" approximation,[1] Kahn and Briat defined the (nonorthogonal) magnetic orbitals Φ_A and Φ_B as the highest occupied molecular orbitals (HOMOs) of the localized A−X and X−B fragments (with the overlap $S_{AB} = \langle\Phi_A|\Phi_B\rangle$), therefore called natural molecular orbitals (NMOs). They then derived the following simple expressions for the exchange coupling constant:

$$J = J_F + J_{AF} \tag{1}$$

with

$$\begin{cases} J_F = 2(j - kS_{AB}^2) \\ J_{AF} \approx -2\dfrac{\Delta S_{AB}}{1 + S_{AB}^2} \end{cases} \tag{2}$$

Δ is (as in the MO formalism) the energy gap between the two A−X−B SOMOs built from the interacting NMOs in the (VB/MO) triplet state. The ferromagnetic j contribution stands as the self-repulsion of the overlap density $\rho_{AB} = \Phi_A\Phi_B$ whereas k is a Coulombic integral involving $\rho_{AA} = \Phi_A^2$.

From a computational point of view, and within the valence-bond, broken-symmetry approach,[7,8] the exchange coupling J ($=J_F + J_{AF}$) can be alternatively written as

$$J = J_F + J_{AF} \approx -2\frac{E_{HS} - E_{BS}}{1 + S_{AB}^2} \tag{3}$$

where E_{HS} and E_{BS} refer to the high-spin (HS: $S = 1$, identified as the triplet) and broken-symmetry (BS: $Ms = 0$) spin states, respectively. In the following, we will use the quantity J_{DFT}, defined as $-2(E_{HS} - E_{BS})$ (i.e., for $S_{AB}^2 \ll 1$, as verified below).

We propose ourselves to present some of the main features of an analytical model attempting to explain the strong ferromagnetism obtained by Ruiz et al. for the planar $[Cu_2(\mu\text{-}O)_2(NH_3)_4]^0$ model cation within the framework of Kahn and Briat's valence bond approach to molecular magnetism. Equation 2 above will be then used as a tool to rationalize our computational results derived from eq 3, in a manner described in the following section.

II.2. Valence Bond Model Revisited. A more explicit VB formulation of J_{AF}, without explicit appearance of Δ (i.e., moving a step backward in Kahn and Briat's derivation) is given by[20]

$$J_{AF} = -\frac{4S_{AB}}{1 - S_{AB}^4}\int\frac{\rho_{AB}(r_1) - S_{AB}\rho_{AA}(r_1)}{r_{B1}}\,d\nu_1 \tag{4}$$

SCHEME 2: Schematic Representation of (Top) the Two Localized Natural Magnetic Orbitals (NMOs) Φ_A and Φ_B, (Middle) the Two Singly Occupied Molecular Orbitals (SOMOs) Ψ_+ and $\Psi-$ in the Triplet State, and (Bottom) the Two Partially Delocalized Orthogonal Magnetic Orbitals (OMOs) Φ_A' and Φ_B'

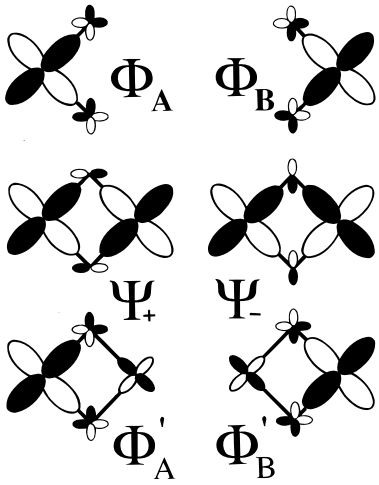

Starting from a simplified description of the NMOs in the case of a di-μ-oxo-bridged Cu(II) dimer (see Scheme 2, top):

$$\begin{cases} \Phi_A = ap_z + bp_x + cd_A \\ \Phi_B = ap_z - bp_x + cd_B \end{cases} \tag{5}$$

with a, b, $c > 0$ and $d_{A,B} \equiv d_{xz}$ (cf. Scheme 1), we obtain (neglecting direct copper d−d overlap):

$$\begin{cases} \langle\Phi_A|\Phi_B\rangle = S_{AB} \approx (a^2 - b^2) + 2c(as_z - bs_x) \\ \langle\Phi_A|\Phi_A\rangle = 1 \approx (a^2 + b^2 + c^2) + 2c(as_z + bs_x) \end{cases} \tag{6}$$

with $s_x = \langle d_A|p_x\rangle = -\langle d_B|p_x\rangle$ and $s_z = \langle d_A|p_z\rangle = \langle d_B|p_z\rangle$ (both negative). From eq 6, we expect at $\theta_C = 90°$, for symmetry reasons, $a = b$, $s_x = s_z$; that is, $S_{AB} = 0$.

If needed, the terminal ligation L can be formally introduced by redefining the metallic $d_{A,B}$ orbitals as monomer orbitals $D_{A,B} \equiv d_{A,B} - L$. Moreover, as the contribution of the bridge s orbitals is usually not negligible, as already shown by HTH,[15] our simplified eq 5 could be easily generalized into

$$\begin{cases} \Phi_A = aP + bS + cD_A \\ \Phi_B = aP - bS + cD_B \end{cases} \tag{7}$$

where P and S now stand for (s, p) bridge orbital combinations ranged according to symmetry (i.e., as they would appear separately in the two SOMOs, i.e., P in $\Phi_A + \Phi_B$, S in $\Phi_A - \Phi_B$). Thus, for the di-μ-oxo-bridged Cu(II) dimer, P would be made out of $\{p_z\}$ (s_z becomes $s_P \equiv \langle D|P\rangle$) and S would be made out of $\{s, p_x\}$ ($s_x = s_S \equiv \langle D|S\rangle$). In particular, $S_{AB} = a^2 - b^2 + 2c(as_P - bs_S)$ no longer cancel for exactly $\theta = 90°$. All our subsequent results could be then easily given in terms of these generalized metal/bridge orbitals, without affecting the form of the analytical expressions derived below. Notice, finally, that the set of eq 7 can be directly used to analyze magneto-structural correlations for any bridged Cu(II) dimers (especially for hydroxo-bridged complexes without modification, or for azido-bridged Cu(II) dimers by setting $S \equiv 0$, as done by us elsewhere[19]).

Coming back to eq 5, the insertion of the analytical expressions of the NMOs into J_{AF} yields the following VB

expression ($S_{AB}^4 \ll 1$):

$$J_{AF} \approx -4S_{AB}\left\{a^2(1-S_{AB})\int\frac{p_z^2(r_1)}{r_{B1}}\,dv_1 - b^2(1+S_{AB})\int\frac{p_x^2(r_1)}{r_{B1}}\,dv_1 - c^2S_{AB}\int\frac{d_A^2(r_1)}{r_{B1}}\,dv_1\right\} + O(s_{x,z}) \quad (8)$$

where $O(s_{x,z})$ stands for all contributing terms involving ($p_{x,z}d_{xz}$) products, whose integrals are of the order of $s_{x,z}$. By restricting therefore J_{AF} to the p^2-bridge[22] and d^2-metal orbitals, the main contributors to J_{AF}, one obtains

$$J_{AF} \approx J_{bdg} + J_{met} \quad (9)$$

where

$$\begin{cases} J_{bdg} \equiv -4S_{AB}\{a^2(1-S_{AB})I_{P_z} - b^2(1+S_{AB})I_{P_x}\} \\ J_{met} \equiv -4S_{AB}\{-c^2S_{AB}I_{D_{xz}}\} \end{cases} \quad (10)$$

and

$$\begin{cases} I_{P_{x,z}} = \int\frac{p_{x,z}^2}{r_{B1}}\,dv_1 \\ I_{D_{xz}} = \int\frac{d_{A,xz}^2}{r_{B1}}\,dv_1 \end{cases} \quad (11)$$

One first notices that the two p_x and p_z orbitals formally contribute separately to J_{bdg} (although both contribute to S_{AB}, of course). If we write $J_{bdg} = J_{bdg}^Z + J_{bdg}^X$, with $J_{bdg}^Z = -4a^2S_{AB}(1-S_{AB})I_{P_z}$ and $J_{bdg}^X = +4b^2S_{AB}(1+S_{AB})I_{P_x}$, one can see that both contributions to J_{bdg} are formally identical, although being of opposite sign, with $J_{bdg}^Z(\theta_C) = J_{bdg}^X(\theta_C) = 0$. Both ferromagnetic and antiferromagnetic contributions are therefore of the same magnitude, and the fact that one will dominate over the other one is a matter of subtle considerations, not easily grasped. In effect, and for symmetry reasons, $I_{P_z}(\theta_C \pm \delta\theta) = I_{P_x}(\theta_C \mp \delta\theta)$. Hence for $\theta < \theta_C$, $a^2 > b^2$, $I_{P_z}(\theta_C - \delta\theta) < I_{P_x}(\theta_C - \delta\theta)$, and $S_{AB} > 0$; that is, there are partial compensations within the products $a^2(1-S_{AB})$ and $b^2(1+S_{AB})$. For $\theta > \theta_C$, $a^2 < b^2$, $I_{P_z}(\theta_C + \delta\theta) > I_{P_x}(\theta_C + \delta\theta)$, and $S_{AB} < 0$.

As far as the order of magnitude is concerned, equating roughly $I_{P_x} \approx I_{P_z} \approx \langle I_P\rangle$ (averaging over θ) and $S_{AB} \approx a^2 - b^2$, one derives a very approximate expression for J_{bdg} (intended for qualitative purposes only):

$$J_{bdg} \approx -4c^2S_{AB}^2\langle I_P\rangle \quad (12)$$

that is, J_{bdg} roughly varies quadratically with S_{AB} (as expected from both HTH and KB since $\Delta \sim S_{AB}$). There is, thus, in J_{bdg}, a partial compensation of the two J_{bdg}^Z and J_{bdg}^X and contributions linear in S_{AB}, and J_{met}, originating from metal d orbitals, is not negligible in comparison, as

$$J_{met} \approx +4c^2S_{AB}^2\langle I_D\rangle \quad (13)$$

This second contribution is found to be always ferromagnetic for the di-μ-oxo-bridged copper(II) dimer, being negligibly small around θ_C but significant (through S_{AB}^2) as θ departs from it.

Finally, equating $J_{AF} \approx J_{bdg} + J_{met}$ with $-2\Delta S_{AB}$ ($S_{AB}^2 \ll 1$) would yield (with $\Delta = \Delta_{bdg} + \Delta_{met}$):

$$\begin{cases} \Delta_{bdg} \approx +2\{a^2(1-S_{AB})I_{P_z} - b^2(1+S_{AB})I_{P_x}\} \\ \Delta_{met} \approx -2c^2S_{AB}I_{D_{xz}} \end{cases} \quad (14)$$

that is, qualitatively (at the same level of eq 12) $\Delta \approx 2c^2S_{AB}(\langle I_P\rangle - \langle I_D\rangle)$. Thus, Δ is linear in S_{AB} as expected.

II.3. Definition of the Quantity $\Delta P^2(d_{xz})$. We now aim at quantifying the VB exchange coupling constant through the use of HS and BS spin populations. This idea relies on the more general goal of being able to relate directly the magnetic properties of a given (triplet) dimer to (for example) its polarized neutron diffraction map measuring the spatial spin density distribution. Spin populations seem to be good intermediates for such a goal. As a clue to the path we followed (the actual scheme has been detailed elsewhere[19]), we very briefly mention two different theoretical results:

i. The first ingredient we use has been obtained by Noodleman within his BS-VB approach.[7] He implicitly showed that $J_{AF} \approx -US_{AB}^2$ (where U is, again, the covalent A−B/ionic A^+−B^- gap, of the order of 5 eV) for weak overlap $S_{AB}^2 \ll 1$. This expression has been computationally verified by Hart et al.[23] Notice already that, as a consequence of both eqs 12 and 13, eq 9 becomes $J_{AF} \approx -4c^2(\langle I_P\rangle - \langle I_D\rangle)S_{AB}^2$, reminiscent of Noodleman's result (more on this below).

ii. The second ingredient has been derived by Caballol et al**.** for metal-only magnetic orbitals, linking qualitatively S_{AB} to copper HS and BS spin populations[16] (their eq 14, i.e., $S_{AB}^2 \approx 1 - P_{BS}^2$ where $P_{HS}^2 = 1$). More generally, it was natural to consider (even when taking into account the bridge) a correlation between J_{AF} and $S_{AB}^2 \approx P_{HS}^2 - P_{BS}^2$ (cf. eq 17 of ref 16). Notice here that, during the peer reviewing of this paper, such a spin population-based estimation of S_{AB}^2 based on both P_{HS} and P_{BS} has been independently published by Ruiz et al.,[24] revisiting Caballol et al.'s previous work.

As a consequence of both ingredients above, we therefore propose to correlate J_{AF} with the quantity $\Delta P^2(d_{xz}) \equiv P_{HS}^2(d_{xz}) - P_{BS}^2(d_{xz})$, that is, $J_{AF} \approx -U\Delta P^2(d_{xz})$. Such a correlation between DFT-computed quantities can be also arrived at by the following analytical reasoning, although with a twist, as we will show that J_{bdg} only (and not J_{AF}) is effectively proportionnal to $\Delta P^2(d_{xz})$ when bridge orbitals are explicitly taken into account.

Let us first construct the symmetrical and antisymmetrical SOMOs of the high-spin (HS), triplet state: $\Psi_\pm = [2(1 \pm S_{AB})]^{-1/2}(\Phi_A \pm \Phi_B)$ (see Scheme 2, middle). These orbitals are then recombined in order to obtain partially delocalized, but mutually orthogonal, monomer orbitals suited for an analysis within the broken symmetry (BS) method as proposed by Noodleman:[7] $\Phi'_{A,B} = 2^{-1/2}(\Psi_+ \pm \Psi_-)$ (see Scheme 2, bottom). We then calculate Mulliken spin populations for the copper ions in the HS and BS states, $P_{HS}(d_{xz})$ and $P_{BS}(d_{xz})$. A guideline of these analytical MO manipulations is proposed in the Appendix (the actual calculation is rather tedious). We then get the following quantity:

$$\begin{aligned} \Delta P^2(d_{xz}) &\equiv P_{HS}^2(d_{xz}) - P_{BS}^2(d_{zz}) \\ &= \frac{c^2S_{AB}}{(1-S_{AB}^2)}\{a^2(1-S_{AB})(1-2s_z^2) - b^2(1+S_{AB})(1-2s_x^2)\} \\ &\approx c^2S_{AB}\{a^2(1-S_{AB}) - b^2(1+S_{AB})\} \end{aligned} \quad (15)$$

as S_{AB}^2, s_x^2, $s_z^2 \ll 1$. The similarity between the expressions of J_{bdg} (eq 10) and $\Delta P^2(d_{xz})$ (eq 15) allows us to expect them to be proportional, through

$$J_{bdg} \approx -\frac{4\langle I_P\rangle}{c^2}\Delta P^2(d_{xz}) \qquad (16)$$

Here is the twist alluded to above: the quantity $\Delta P^2(d_{xz})/c^2$ (and not $\Delta P^2(d_{xz})$ in this particular case) provides us with a mean of quantifying J_{bdg} (and not J_{AF} as first expected) within the KB-VB approach. The appearance of the factor c^2 in J_{bdg} results from the fact of having *two* orthogonal p orbitals mediating the exchange phenomenon. Only in the conditions in which Noodleman's VB-BS formalism strictly applies, that is $a, b \ll 1$ (i.e., $c^2 \approx 1$), would $\Delta P^2(d_{xz})$ equate $S_{AB}{}^2$. Then, and only then, $J_{AF} \approx J_{bdg} + J_{met} \approx -4(\langle I_P\rangle - \langle I_D\rangle)S_{AB}{}^2$. This last equation would be the transcription, within our approach, of Noodleman's result,[7] with, formally, $U \equiv 4(\langle I_P\rangle - \langle I_D\rangle)$. It is therefore important to stress that Noodleman obtained his expression for J_{AF} at the (metal only) superexchange level (see ref 25 for the inclusion of metal-bridge contributions), although it should still hold as long as the weight of the bridging orbitals in the magnetic orbitals is small (i.e., fulfilling the "active electron" approximation[1]).

III. Density Functional Study

III.1. Quantum Chemistry Codes. Our calculations make use of the Amsterdam LCAO density-functional program (ADF 2.3) developed by Baerends and co-workers.[17,18,26−29] We used the exchange-correlation "VBP" potential (Vosko, Wilk, and Nusair's exchange and correlation energy[30,31] completed by nonlocal gradient corrections to the exchange by Becke[32] as well as to the correlation by Perdew[33]). We used, moreover, triple-ζ (plus polarization) basis sets for all atoms. As already hinted at above, we slightly modified the original ADF triple-ζ copper basis set, spatially contracting it, as fully discussed and justified elsewhere.[19]

III.2. Results. We considered the case of the planar $[Cu^{II}{}_2(\mu\text{-}O^{2-})_2(NH_3)_4]^0$ cation, as done by Ruiz et al.[6] (cf. Scheme 1). Some calculated quantities relevant for our discussion are reported in Table 1. The overlap S_{AB} (as it appears in Table 1) has been computed from a, b, c, s_x and s_z values as they appear in the BS state: the singly occupied MO for each spin represents well the NMO (coefficients reported in Table S-1, Supporting Information).

We show in Figure 1 (filled circles, ●) the plot of J_{DFT} as a function of θ comprised between 70° and 110° (including the two angles 96° and 101° used in ref 6). J_{DFT} is mostly ferromagnetic, moreover increasing in magnitude over most of the angle range. This odd result, whose discussion is shifted to section IV, is in contrast, as to the sign of the slope of $J_{DFT}(\theta)$, but not as to the sign of J_{DFT} itself, with Figure 1 of Ruiz et al.[6] They specifically considered in their Figure 1 an octahedral ligand coordination on the copper sites, against a planar one in our case. We find, however, the same large ferromagnetism. We notice also in our Figure 1 that J_{DFT} presents two inflections, one around $\theta \approx 75°$, and a second one near 105° (more on this below).

Next, it can be easily shown that $J_{DFT}(\theta)$ here obtained is not compatible with a constant J_F term and a varying J_{AF} term in the MO sense. In effect, the two SOMOs become degenerate for $\theta_C \approx 96°$ (not 90°, because of the actual involvement of s bridge orbitals, as discussed by HTH[15]). For smaller and larger angles, Δ keeps increasing in magnitude as θ departs from θ_C (Δ changes its sign at θ_C, as already noticed by Ruiz et al.[6]). But, for larger angles, the total exchange coupling constant J_{DFT} is still increasingly ferromagnetic, and one cannot argue there

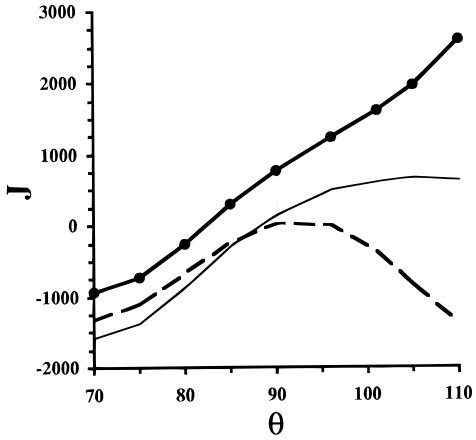

Figure 1. Plot of J_{DFT} (in cm^{-1}) as a function of the Cu−O−Cu bond angle θ. The thin continuous line stands for $J_{bdg} \approx -k\Delta P^2(d_{xz})/c^2$ (with $k \approx 16\,000$ cm^{-1}; see main text). The dashed line stands for $-2\Delta S_{AB}$ (see main text).

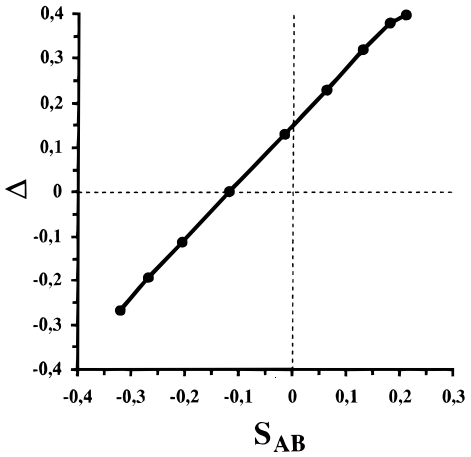

Figure 2. Plot of Δ (as calculated by DFT) as a function of S_{AB} (given in Table 1).

TABLE 1: J_{DFT} (in cm^{-1}), SOMO Gap Δ (in eV), Estimated S_{AB}, $P_{HS/BS}(d_{xz})$, and $\Delta P_{DFT}{}^2(d_{xz})$ as a Function of the Cu−O−Cu Bond Angle θ

θ, deg	J_{DFT} (cm^{-1})	Δ (eV)	S_{AB}	$P_{HS}(d_{xz})$	$P_{BS}(d_{xz})$	$\Delta P_{DFT}{}^2(d_{xz})$
70	−934	+0.395	+0.209	0.4690	0.4279	+0.037
75	−729	+0.379	+0.180	0.4757	0.4396	+0.033
80	−248	+0.318	+0.129	0.4759	0.4535	+0.021
85	+300	+0.230	+0.063	0.4701	0.4627	+0.007
90	+776	+0.130	−0.014	0.4582	0.4630	−0.004
96	+1246	+0.002	−0.117	0.4347	0.4487	−0.012
101	+1604	−0.113	−0.205	0.4075	0.4247	−0.014
105	+1964	−0.193	−0.268	0.3796	0.3975	−0.014
110	+2598	−0.267	−0.320	0.3392	0.3565	−0.012

that the antiferromagnetic contribution is increasing proportionally to $-\Delta^2/U$.

The same kind of remark could be addressed to the VB model, as developed initially by Kahn and Briat.[20,21] Assuming again a constant J_F, it remains to quantify the differential antiferromagnetic contribution as $-2\Delta S_{AB}$ (cf. eq 2). If this model explains well our results for $\theta < \theta_C$ (see the dashed line on Figure 1), it does not for $\theta > \theta_C$ (Δ and S_{AB} being of the same sign: cf. Table 1 and Figure 2, where one verifies the linear relationship between both quantities). We explicitly verified that Δ and S_{AB} are most often of the same sign (except just around θ_C as $\Delta \approx 0$ for $\theta \approx 96°$ whereas $S_{AB} \approx 0$ for $\theta \approx 90°$; cf. Figure 2). Incidentally, that Δ and S_{AB} do not necessarily cancel for exactly the same set of structural parameters has already

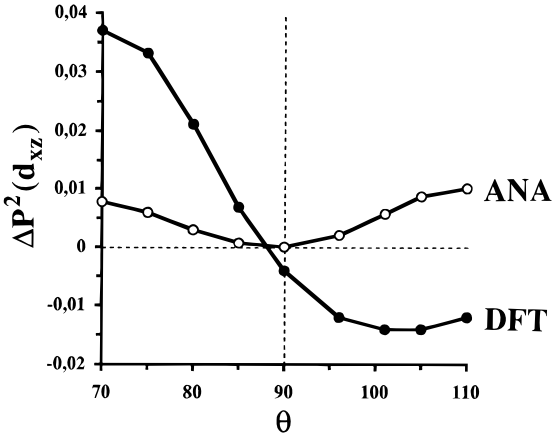

Figure 3. Plot of $\Delta P_{DFT}^2(d_{xz})$ (filled circles, ●) and $\Delta P_{ANA}^2(d_{xz})$ (open circles, ○) as a function of the Cu−O−Cu bond angle θ.

been noticed by others.[34] Interestingly, therefore, for θ in the range 90−96°, this provides for a small ferromagnetic contribution as $-2\Delta S_{AB}$ (supposedly antiferromagnetic) becomes actually ferromagnetic.

Either way, we see that there must be some variable (and important) ferromagnetic contribution to J_{DFT} for $\theta \geq \theta_C$ as the conventional HTH-MO or KB-VB molecular magnetism models cannot rationalize our computational results.

Turning now to our alternative formulation (cf. eq 16) of Kahn and Briat's VB approach,[19] there are two ways to proceed further, depending on how one computes $\Delta P^2(d_{xz})$'s.

On one hand, one can compute $\Delta P^2(d_{xz})$ analytically (cf. eq 15) from the *a*, *b*, *c*, s_x and s_y parameters listed in Table S-1 (results given under the heading $\Delta P_{ANA}^2(d_{xz})$ in Table S-1). It can be easily seen that $J_{bdg} \approx -4\langle I_P\rangle \Delta P_{ANA}^2(d_{xz})/c^2$ (or, for that matter, $J_{bdg} + J_{met}$) will assume a variation similar to that of $-\Delta^2/U$, $-2\Delta S_{AB}$ or $-US_{AB}^2$ (see open circles (○) in Figure 3). Notice in particular that $\Delta P_{ANA}^2(d_{xz}) \geq 0$, canceling only around θ_C. This serves only to illustrate the consistency of our spin population-based approach as we started our derivation from $J_{AF} \approx -2\Delta S_{AB}$. This shows also that $\Delta P_{ANA}^2(d_{xz})$ cannot serve to rationalize $J_{DFT}(\theta)$ as computed by us.

On the other hand, the DFT-computed d_{xz} HS and BS spin populations yield an alternative estimation of $\Delta P^2(d_{xz})$, now called $\Delta P_{DFT}^2(d_{xz})$, plotted as filled circles (●) in Figure 3. As can be seen there, $|\Delta P_{DFT}^2(d_{xz})| > |\Delta P_{ANA}^2(d_{xz})|$ with $\Delta P_{DFT}^2(d_{xz})$ canceling around 90°. Most importantly, however, $\Delta P_{DFT}^2(d_{xz})$ becomes *negative* for $\theta \geq \theta_C$ (i.e., $P_{HS}(d_{xz}) < P_{BS}(d_{xz})$: cf. Table 1). A tentative reason will be given below in section IV. Consequently, $J_{bdg} \approx -4\langle I_P\rangle \Delta P_{DFT}^2(d_{xz})/c^2$, and therefore $J_{AF} \approx J_{bdg} + J_{met}$ actually turn out ferromagnetic!

We thus plotted J_{DFT} as a function of $\Delta P_{DFT}^2(d_{xz})/c^2$ (filled circles (●) in Figure 4). For $\theta \leq \theta_C$, the plot is about linear, with a slope of ~10 600 cm^{-1} (2 eV). A roughly constant J_F value will not affect much the estimation of the slope. We also plotted in Figure 4 (open circle, ○) J_{DFT} as a function of Δ^2, only to verify that both quantities are indeed linearly related for $\theta \leq \theta_C$. We then extrapolated this linear behavior observed for small angles to large angles, reporting a plot of $J_{bdg}(cm^{-1}) \approx -16\,000.\Delta P_{DFT}^2(d_{xz})/c^2$ (thin continuous line) in Figure 1. The remaining difference between J_{DFT} and J_{bdg} could be explained, for $\theta \leq \theta_C$, by a roughly constant "true" ferromagnetic term ($J_F \sim 700$ cm^{-1}). But the key point to understand the difference between J_{DFT} and $J_F + J_{bdg}$ for large angles now lies in the additional ferromagnetic term J_{met} mentionned in section II.1. The quantity $4c^2S_{AB}^2$, proportional to J_{met}, is reported in Figure 5. As one can see there, $J_{met}(\theta_C + \delta\theta) \geq 2J_{met}(\theta_C - \delta\theta)$ (where $\delta\theta \geq 0$): this additional ferromagnetic effect is therefore enhenced for $\theta \geq \theta_C$.

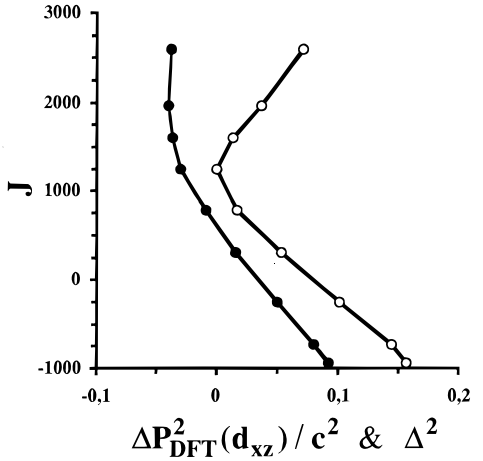

Figure 4. Plots of J_{DFT} as a function of $10\Delta P_{DFT}^2(d_{xz})$ (filled circles, ●) or Δ^2 (open circles, ○).

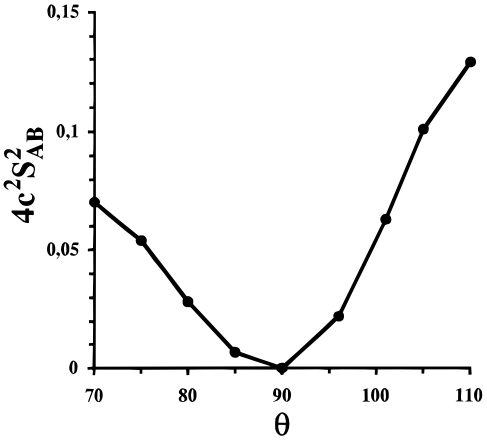

Figure 5. Plot of J_{met} (through that of the quantity $4c^2S_{AB}^2$) as a function of the Cu−O−Cu bond angle θ.

To obtain simultaneously reliable estimations of both $\langle I_P\rangle$ and $\langle I_D\rangle$, we tentatively fitted $J_{DFT}(\theta)$ (in the least-squares sense) with the function J_{OPT} defined in eq 17, where J_F, $\langle I_P\rangle$, and $\langle I_D\rangle$

$$J_{OPT} \approx \mathbf{J}_F - 4\langle \mathbf{I}_P\rangle\left(\frac{\Delta P_{DFT}^{\ 2}(d_{xz})}{c^2}\right) + 4\langle \mathbf{I}_D\rangle c^2 S_{AB}^{\ 2} \quad (17)$$

are treated as parameters (averaged over θ) to be optimized, although neither of the three is strictly constant. We found for the whole θ range $J_F \approx 500$ cm^{-1}, $\langle I_P\rangle \approx 5200$ cm^{-1}, and $\langle I_D\rangle \approx 8100$ cm^{-1} (J_{DFT} is plotted against J_{OPT} in Figure S-1, Supporting Information). Limiting the same fit to $\theta \leq 90°$ yields rather $J_F \approx 600$ cm^{-1}, $\langle I_P\rangle \approx 4600$ cm^{-1}, and $\langle I_D\rangle \approx 2400$ cm^{-1}. This would set up an upper limit to $J = J_F + J_{AF}$ of 500−600 cm^{-1}, if J_{AF} would remain negative according to classical molecular magnetism models. No value of *U* can be estimated from these parameters (here $U \equiv 4(\langle I_P\rangle - \langle I_D\rangle) < 0$ when the whole θ range is used!). Let us restate here that we do not satisfy Noodleman's approximations (here translated into $c^2 \approx 1$) to obtain reliable *U* values (cf. end of section II.3). Stated otherwise, it is not possible to fit our computed $J_{DFT}(\theta)$ values with a function of the form $J_F - US_{AB}^2$ for the whole θ range (although, for $\theta \leq \theta_C$, $J_{AF} \approx -US_{AB}^2$ would yield *U* between 4 and 5 eV, in relative good agreement with 6.5 eV obtained from photoelectron spectroscopy for copper chlorides[35] or 5.9 eV, Anderson's estimate[36]).

IV. Discussion and Conclusion

For $\theta \leq \theta_C$, our DFT results on the $[Cu_2(\mu\text{-}O)_2(NH_3)_4]^0$ cation can be rationalized by the classical molecular magnetism models currently available. This is not the case for $\theta \geq \theta_C$: this system seems to be exceptional because of its large remanent and increasing ferromagnetism beyond θ_C. But, as noted by a referee, this result is in contradiction with the classical magneto-structural correlation reported early by Crawford et al. for the analogous (cf. section II.2) hydroxo-bridged Cu(II) complexes[4] exhibiting an increase of the antiferromagnetic contribution beyond θ_C.

On one hand, this surprising behavior can still be understood on the basis of our modified VB approach, using, however, $\Delta P_{DFT}^2(d_{xz})$ rather than $\Delta P_{ANA}^2(d_{xz})$ values. This amounts to saying that the supposedly VB antiferromagnetic term $J_{AF} \approx J_{bdg} + J_{met}$ then turns out to be ferromagnetic, mainly because of *negative* $\Delta P_{DFT}^2(d_{xz})$'s for large angles. This therefore manifests a certain level of consistency between DFT-computed J_{DFT} and $\Delta P_{DFT}^2(d_{xz})$ quantities.

On the other hand, by identifying the VB NMOs as the singly occupied α and β broken symmetry MOs, we obtained a set of parameters yielding *positive* $\Delta P_{ANA}^2(d_{xz})$ values (cf. Figure 3 and Table S-1). These last values behave for the whole angle range as expected on the basis of classical HTH-MO, KB-VB, or BS-VB models but cannot explain our computational results for large angles.

Where is the trick ?

To help solve this puzzle, we calculated P_{HS} and P_{BS} (analytical expressions given in eq A-3 of the Appendix) using the BS *a*, *b*, *c*, s_x and s_z, and *c* parameters listed in Table S-1 and compare them with DFT-based values (given in Table 1). If DFT P_{HS} values are rather well predicted (except around $\theta \approx 70°$; cf. Figure 6a), such is not the case for the P_{BS} quantities (cf. Figure 6b).

As one performs a Mulliken spin population analysis on the DFT-computed triplet state, the two SOMOs (Ψ_+ and Ψ_-) turn out to be the only source of P_{HS} (we mean that there is no net spin population arising from the doubly occupied spin−orbitals). In other words, the "active electron" approximation[1] is there valid. In the BS state, however, ∼30% of the spin population actually originates from the doubly occupied (polarized) spin−orbitals, below the two BS-NMOs, over the whole θ range. Therefore, the culprit at the heart of the puzzle mentionned above seems to be the DFT-computed BS copper spin populations P_{BS} (and therefore the BS spin state itself). The behavior of $\Delta P_{DFT}^2(d_{xz})$ and $\Delta P_{ANA}^2(d_{xz})$ for $\theta \geq \theta_C$ are thus mutually inconsistent, being both of opposite signs. The remarkable point is still that the computed J_{DFT} values behave consistently with $\Delta P_{DFT}^2(d_{xz})$ (as a consequence of eq 16), although the predicted strong ferromagnetism is most probably artifactual.

Furthermore, both oxygen atoms start to interact through the p_x orbital used in the NMOs (cf. eq 5). This (antibonding) $p_x \equiv p_x^+$ orbitals actually stands as a normalized bridge orbital, (i.e., $p_x^{\pm} = (2 + 2\sigma)^{-1/2}(p_x^t \pm p_x^b)$, where "t" and "b" refer to the two oxygen atoms, and $\sigma = \langle p_x^t | p_x^b \rangle < 0$). For $\theta \leq \theta_C$, the bonding−antibonding p_x^+/p_x^- gap is about constant and small (≈0.5 eV) so that the electronegative bridge orbital lies below that of the metal. As θ increases above θ_C, this gap increases up to ≈2.5 eV for $\theta = 110°$, the p_x orbital raising higher than the Cu d_{xz} orbitals. The corresponding SOMO Ψ_- in the triplet state thus becomes mainly oxygen in character; that is, one goes formally from the $Cu^{II}_2(O^{2-})_2$ configuration (for $\theta < \theta_C$) to the $Cu^{I}_2(O^{-})_2$ configuration (for $\theta > \theta_C$), resulting in both the lowering of $P_{HS}(d_{xz})$ (Cu(II) → Cu(I); cf. Figure 6a) and the parallel increase of the O spin population ($O^{2-} \rightarrow O^{-}$; not shown) in the triplet (HS) state. In the BS state, however, the magnetic orbitals turn out to be more localized on each left anf right fragments and $\Delta P_{DFT}^2(d_{xz})$ actually becomes negative as a consequence.

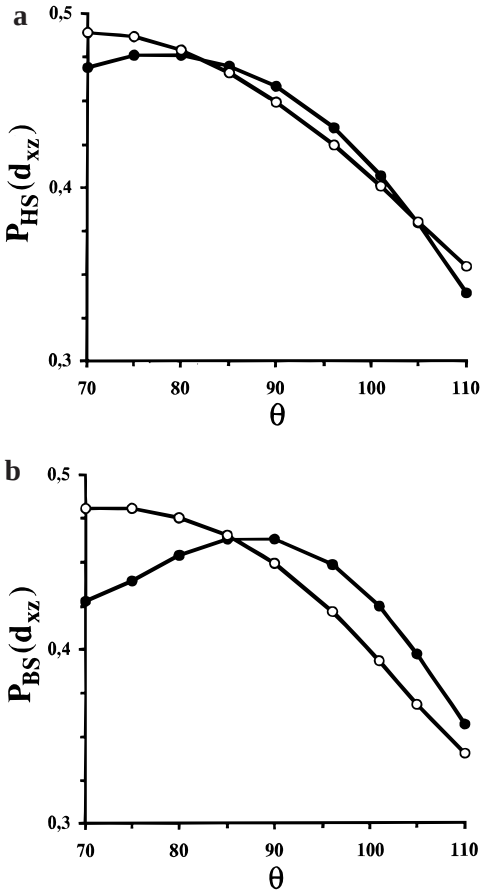

Figure 6. Plots of DFT-based (filled circles, ●) and analytical (open circles, ○) $P_{HS}(d_{xz})$ (a) and $P_{BS}(d_{xz})$ (b) as a function of the Cu−O−Cu bond angle θ.

Of course, this change from $Cu^{II}_2(O^{2-})_2$ to $Cu^{I}_2(O^{-})_2$ is but a trend. In $Cu^{II}_2(O^{-})_2$ (not Cu(I) though), d(O−O) ≈ 1.4 Å (see for example ref 11), whereas for $\theta = 110°$, d(O−O) ≈ 2.3 Å in our model dimer. We are thus far from a typical peroxo O−O distance. Upon actually reaching the $Cu^{I}_2(O^{-})_2$ configuration (for $\theta \approx 140°$, corresponding to d(O−O) ≈ 1.4 Å), one would expect J to revert toward diamagnetism (Cu(I) and O_2^{2-} being both diamagnetic). Computationally, however, we did not verify that point.

As a conclusion, we developed in section II a spin population-based model linking analytically J_{bdg}, the main contributor to J_{AF}, to the quantity $\Delta P_{ANA}^2(d_{xz})$ (cf. eq 16). At this level, our theoretical formulation of molecular magnetism is fully compatible with other classical models. Computationally, however, J_{bdg} (as well as J_{AF}) becomes ferromagnetic for $\theta > \theta_C$ because of negative $\Delta P_{DFT}^2(d_{xz})$ values. It is then remarkable that J_{DFT} actually follows such a prediction. The DFT computations are thus internally consistent, as is the analytical model, although both differ radically as far as the resulting magnetism of the dimer is concerned.

We therefore wonder if the exchange coupling constant of the $[Cu_2(\mu\text{-}O)_2(NH_3)_4]^0$ cation, predicted to be strongly ferromagnetic by us and others,[6] corresponds to the reality of actual di-μ-oxo-bridged copper dimers. Without dividing $J = J_F + J_{AF}$ by 2, Ruiz et al. would find a ferromagnetic exchange coupling constant of almost 2000 cm^{-1}, whereas our own work sets up an upper limit of about 500−600 cm^{-1} (if one accepts

the value of J_F obtained from eq 17 as being correct, apart from the unexpected behavior of J_{AF}). In our view, this surprising result is most probably linked (fully or partially) to a computational artifact at the BS state level. In effect, the required conditions for a proper use of the BS techniques in this particular case are not satisfied (cf. end of sections II.3 and III.2). Although the magnetic orbital overlap S_{AB} is small ($S_{AB}^2 \ll 1$), this is not because the *weight* of the bridging orbitals $\{p_x, p_z\}$ in Φ_A and Φ_B is small (i.e., $a, b \ll 1$ in eq 5 or 7, thus fulfilling the "active electron" approximation), but because there is partial *compensation* between both p_x/p_z contributions in $S_{AB} \approx a^2 - b^2$ (cf. eq 6), hence the occurrence of additional c^2 factors in eqs 12−13 and 15−17.

However, the quantity $\Delta P_{DFT}^2(d_{xz})$ remains a remarkably simple tool for the estimation of DFT-computed exchange coupling constants, as demonstrated in sections II and III (see also ref 19 for further details). This provides an alternative semiquantitative way, to that of HTH, of rationalizing the exchange phenomenon, although it requires the convergence of two (HS and BS) instead of one (HS only) spin states.

Acknowledgment. We thank the *Commissariat à l'Energie Atomique* for the use of the CRAY-94 supercomputer in Grenoble.

Appendix

Within the framework of the oxo-bridged dimer defined in section II.2, and from the two localized fragment orbitals Φ_A and Φ_B, one constructs two (symmetric and antisymmetric) SOMOs, typical for a HS-type calculation:

$$\begin{cases} \Psi_+ = \dfrac{1}{\sqrt{2(1+S_{AB})}}[\Phi_A + \Phi_B] = \\ \qquad \dfrac{1}{\sqrt{(1+S_{AB})}}\left[2a\dfrac{p_z}{\sqrt{2}} + c\dfrac{d_A + d_B}{\sqrt{2}}\right] \\ \Psi_- = \dfrac{1}{\sqrt{2(1-S_{AB})}}[\Phi_A - \Phi_B] = \\ \qquad \dfrac{1}{\sqrt{(1-S_{AB})}}\left[2b\dfrac{p_x}{\sqrt{2}} + c\dfrac{d_A - d_B}{\sqrt{2}}\right] \end{cases} \quad \text{(A-1)}$$

We now want to recombine these two MOs in order to obtain (mutually orthogonal) monomer orbitals partly delocalized onto the other metal:

$$\begin{aligned} \Phi'_A &= \frac{1}{\sqrt{2}}[\Psi_+ + \Psi_-] \\ &= \frac{1}{2}\left[\frac{2ap_z}{\sqrt{(1+S_{AB})}} + \frac{2bp_x}{\sqrt{(1-S_{AB})}} + c\left(\frac{1}{\sqrt{(1+S_{AB})}} + \frac{1}{\sqrt{(1-S_{AB})}}\right)d_A + c\left(\frac{1}{\sqrt{(1+S_{AB})}} - \frac{1}{\sqrt{(1-S_{AB})}}\right)d_B\right] \\ \Phi'_B &= \frac{1}{\sqrt{2}}[\Psi_+ - \Psi_-] \\ &= \frac{1}{2}\left[\frac{2ap_z}{\sqrt{(1+S_{AB})}} - \frac{2bp_x}{\sqrt{(1-S_{AB})}} + c\left(\frac{1}{\sqrt{(1+S_{AB})}} - \frac{1}{\sqrt{(1-S_{AB})}}\right)d_A + c\left(\frac{1}{\sqrt{(1+S_{AB})}} + \frac{1}{\sqrt{(1-S_{AB})}}\right)d_B\right] \end{aligned} \quad \text{(A-2)}$$

This new set of orbitals correspond to the two monomer (partially delocalized) functions after mutual interaction, as suited within the broken symmetry method. We then calculate the Mulliken copper spin populations ($P_A(d_A)$ for Cu_A in Φ'_A and $P_B(d_A)$ for Cu_A in Φ'_B). Consequently, we finally compute the HS (i.e., P_{HS}) and the BS (i.e., P_{BS}) spin populations as

$$\begin{cases} P_{HS}(d_A) = P_A(d_A) + P_B(d_A) = \dfrac{c^2 + acs_z(1 - S_{AB}) + bcs_x(1 + S_{AB})}{1 - S_{AB}^2} \\ P_{BS}(d_A) = P_A(d_A) - P_B(d_A) = \dfrac{c^2 + acs_z + bcs_x}{\sqrt{1 - S_{AB}^2}} \end{cases} \quad \text{(A-3)}$$

An analytical expression for $\Delta P^2(d_{xz})$ is then straightforwardly derived, given in the main text (eq 15).

Supporting Information Available: Plot of J_{DFT} against J_{OPT} and table of coefficients for the singly occupied MO. This information is available free of charge via the Internet at http://pubs.acs.org.

References and Notes

(1) Kahn, O. *Molecular Magnetism*; VCH Publishers: New York, 1993.
(2) Aebersold, M. A.; Gillon, B.; Plantevin, O.; Pardi, L.; Kahn, O.; Bergerat, P.; vonSeggern, I.; Tuczek, F.; Öhtröm, L.; Grand, A.; Lelièvre-Berna, E. *J. Am. Chem. Soc.* **1998**, *120*, 5238−5245.
(3) Ruiz, E.; Cano, J.; Alvarez, S.; Alemany, P. *J. Am. Chem. Soc.* **1998**, *120*, 11122.
(4) Crawford, W. H.; Richardson, H. W.; Wasson, J. R.; Hodgson, D. J.; Hatfield, W. E. *Inorg. Chem.* **1976**, *15*, 2107.
(5) Ruiz, E.; Alemany, P.; Alvarez, S.; Cano, J. *Inorg. Chem.* **1997**, *36*, 3683−3688.
(6) Ruiz, E.; Alvarez, S.; Alemany, P. *Chem. Commun.* **1998**, 2767−2768.
(7) Noodleman, L. *J. Chem. Phys.* **1981**, *74*, 5737−5743.
(8) Noodleman, L.; Case, D. A. *Adv. Inorg. Chem.* **1992**, *38*, 423−470.
(9) Frisch, M. J.; et al. *Gaussian 94*; Gaussian, Inc.: Pittsburgh, PA, 1994.
(10) Tuczek, F.; Solomon, E. I. *J. Am. Chem. Soc.* **1994**, *116*, 6916−6924.
(11) Tolman, W. B. *Acc. Chem. Res.* **1997**, *30*, 227−237.
(12) Flock, M.; Pierloot, K. *J. Phys. Chem. A* **1999**, *103*, 95−102.
(13) Zang, Y.; Dong, Y.; Que, L.; Kauffmann, K.; Münck, E. *J. Am. Chem. Soc.* **1995**, *117*, 1169−1170.
(14) McGrady, J. E.; Stranger, R. *J. Am. Chem. Soc.* **1997**, *119*, 8512−8522.
(15) Hay, P. J.; Thibeault, J. C.; Hoffmann, R. *J. Am. Chem. Soc.* **1975**, *97*, 4884−4899.
(16) Caballol, R.; Castell, O.; Illas, F.; Moreira, P. R.; Malrieu, J. P. *J. Phys. Chem. A* **1997**, *101*, 7860.
(17) Baerends, E. J.; Ellis, D. E.; Ros, P. *Chem. Phys.* **1973**, *2*, 41−51.
(18) teVelde, G.; Baerends, E. J. *J. Comput. Phys.* **1992**, *99*, 84−98.
(19) Blanchet-Boiteux, C.; Mouesca, J.-M. *J. Am. Chem. Soc.* **2000**, *122*, 861−869.
(20) Kahn, O.; Briat, B. *J. Chem. Soc. Trans. 2* **1976**, *72*, 268.
(21) Kahn, O.; Briat, B. *J. Chem. Soc. Trans. 2* **1976**, *72*, 1441.
(22) Kahn, O.; Charlot, M. F. *Nouv. J. Chim.* **1980**, *4*, 567−576.
(23) Hart, J. R.; Rappé, A. K.; Gorun, S. M.; Upton, T. H. *J. Phys. Chem.* **1992**, *96*, 6255−6263.
(24) Ruiz, E.; Cano, J.; Alvarez, S.; Alemany, P. *J. Comput. Chem.* **1999**, *20*, 1391−1400.
(25) Noodleman, L.; Davidson, E. R. *Chem. Phys.* **1986**, *109*, 131−143.
(26) Baerends, E. J.; Ros, P. *Chem. Phys.* **1973**, *2*, 52−59.
(27) Baerends, E. J.; Ros, P. *Int. J. Quantum Chem., Quantum Chem. Symp.* **1978**, *12*, 169−190.
(28) Bickelhaupt, F. M.; Baerends, E. J.; Ravenek, W. *Inorg. Chem.* **1990**, *29*, 350−354.
(29) Ziegler, T. *Chem. Rev.* **1991**, *91*, 651−667.
(30) Vosko, S. H.; Wilk, L.; Nusair, M. *Can. J. Phys.* **1980**, *58*, 1200.
(31) Painter, G. S. *Phys. Rev.* **1981**, *B24*, 4264−4270.
(32) Becke, A. D. *Phys. Rev.* **1988**, *A38*, 3098−3100.
(33) Perdew, J. P. *Phys. Rev.* **1986**, *B33*, 8822−8824.
(34) VanKalkeren, G.; Schmidt, W. W.; Block, R. *Physica* **1979**, *97B*, 315.
(35) Didziulis, S. V.; Cohen, S. L.; Gewirth, A. A.; Solomon, E. I. *J. Am. Chem. Soc.* **1988**, *110*, 250.
(36) Anderson, P. W. *Phys. Rev.* **1959**, *115*, 2−13.